A Study of Landscape Generated Moist Convection. Impact of Soil Patches and Atmospheric Boundary Conditions on Precipitation and Soil Moisture Distribution

Wei-Kuo Tao[1] and Barry H. Lynn[2]

[1]NASA/Goddard Space Flight Center
[2]Universities Space Research Association
NASA/Goddard Space Flight Center
Greenbelt, Maryland
USA

Abstract

A two-dimensional cloud resolving model was used to study the impact of soil moisture patches and atmospheric boundary conditions on cloud structure, rainfall, and soil moisture distribution. Dry and moist patches in the simulation domain experienced quite different heat fluxes. Mesoscale circulations generated by the contrast in surface sensible heat flux triggered deep moist convection, which propagated along sea-breeze like fronts. In contrast, only relatively weak, but widespread and shallow moist convection occurred over domains in which the patches were quite small. The results suggested a significant, systematic impact of patch size and background wind on moist convection, including cloud structure and rainfall, and the recycling of water - effects which parameterizations of deep moist convection might need to include. The impact of rainfall interception and reevaporation on developing moist convection was small. However, this convection created large rainfall *footprints*. These footprints resulted in new moist patches, altering quite dramatically the distribution of soil moisture after *one* day of model simulation. Thus, new statistical representations of subgrid-scale landscape properties are needed for GCMs, which account for the time dependent nature of patch size and soil moisture.

1. INTRODUCTION

Satellite observations show that meteorologically significant landscape discontinuities of soil type, soil wetness, vegetation cover, water bodies, and topography are found across vast land areas (Olsen et al., 1983; Henderson-Sellers *et al*, 1988; Avissar, 1991; Pielke *et al*, 1991; and Avissar and Chen, 1994). Thus, it is not surprising that observations suggest the existence of landscape-generated mesoscale circulations associated with landscape patches defined by these discontinuities (Doran *et al*, 1995). These circulations are generated by contrasts in surface heat fluxes that can occur, for example, between relatively wet and dry ground.

Analytical and numerical studies have shown that landscape generated mesoscale circulations can assume the form of strong sea breezes (Anthes, 1984; Pielke *et al*, 1991; Avissar and Chen, 1993; Lynn *et al*, 1995a), and that circulations associated with patches with length scale similar to the Rossby radius of deformation are most intense. Most importantly, both observational and numerical results suggest that mesoscale circulations generated by landscape patches can affect

the formation of shallow clouds (Chen and Avissar, 1994; Hong *et al*, 1995).

The GEWEX Continental-Scale International Project seeks to develop improved models and parameterizations of physical processes associated with the transfer of heat, moisture, and momentum across the land/atmospheric interface through the atmospheric boundary layer into the free atmosphere. Particular emphasis is placed on issues involving the scale integration of these processes for climate models. Thus, the continued study of the interactions of soil moisture discontinuities and atmosphere on moist convection seems appropriate. Moreover, prior work has been limited to cases of shallow convection produced with a constant background wind over individual patches.

In this study, a two-dimensional cloud resolving model was used to simulate deep convection in the presence of wind shear. It was used to explicitly resolve the land surface and convective clouds, and there was explicit two-way interaction between both. The initial atmospheric profiles for this study were obtained from the Convective and Electrification Precipitation experiment (CaPE). The atmosphere was characterized by a weak vertical wind shear and small Convective Available Potential Energy (CAPE). However, a large CAPE developed in response to diurnal heating and moistening of the planetary boundary layer by the surface heat fluxes.

2. METHOD

2.1 Cumulus Ensemble Model

The model used in this study is the Goddard Cumulus Ensemble Model (GCE; Tao and Simpson, 1993). It has been extensively applied to explicitly represent cloud-environment interactions, cloud interaction and mergers, air-sea interaction, cloud draft structure and trace gas transport (Fig. 1). The model includes solar and infrared radiative transfer processes, and explicit cloud-radiation interaction processes. The cloud microphysics include a parameterized Kessler-type two-category liquid water scheme (cloud water and rain). It has two parameterizations of a three-category ice phase scheme (cloud ice, snow, and hail/graupel) (Lin *et al*, 1983; and Rutledge and Hobbs, 1984).

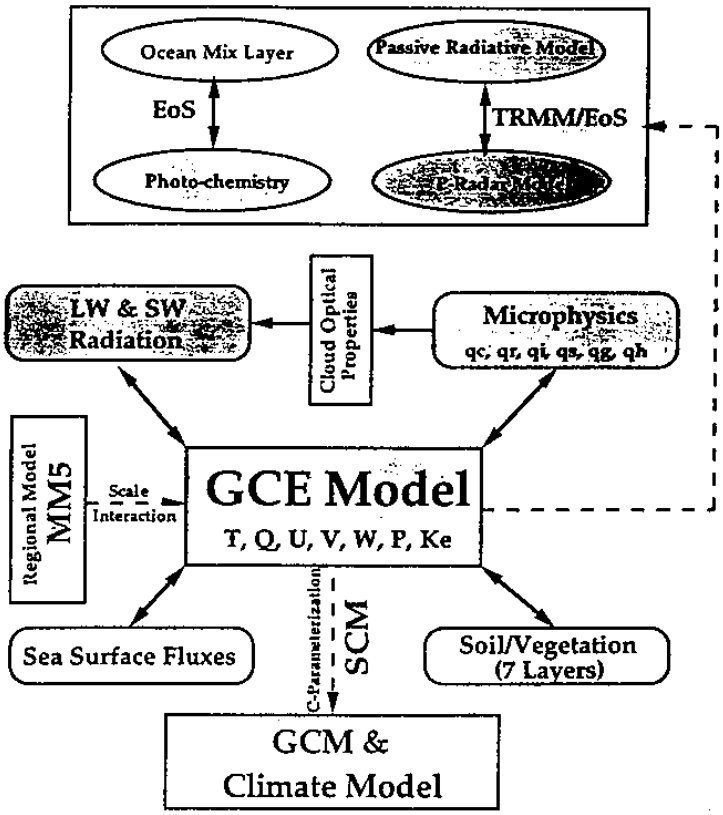

Fig.1 Schematic diagram demonstrating the characteristics of GCE model. Arrow with solid line indicates a two-way interaction among different physical processes and arrow with dashed line indicates an one-way interaction. (SCM - Single Column Model)

The atmospheric model was recently modified to include a land-surface parameterization scheme described by Wetzel and Boone (1995), which provides state-of-the-art representation of land surface processes (Fig. 2). In brief, PLACE

(Parameterization for Land-Atmosphere-Cloud Exchange) is a land-surface model developed by Wetzel and Boone (1996). The PLACE is a soil-vegetation model that accounts for detailed, interactive processes between a partly cloudy atmospheric boundary layer model and underlying heterogeneous land surfaces (Fig. 2). It basically consists of two process modules coupled to a bulk (one layer) boundary layer parameterization. The soil module contains seven water reservoirs, and the cloud parcel module determines atmospheric boundary layer stratification (this cloud module is turned-off when the PLACE is linked with the GCE model). The soil module includes plant internal storage, dew and intercepted precipitation, surface material (no roots), top-soil layer, subsoil layer, and two deeper layers consisting of a base layer and a deep soil layer that regulate seasonal and interannual availability of water. At the soil surface, the soil water infiltration method described by Boone and Wetzel (1996) was implemented. The flux of heat into the soil is dependent upon a thermal conductivity (McCumber and Pielke, 1981), which accounts for both the soil texture and water content. Intercomparisons have demonstrated

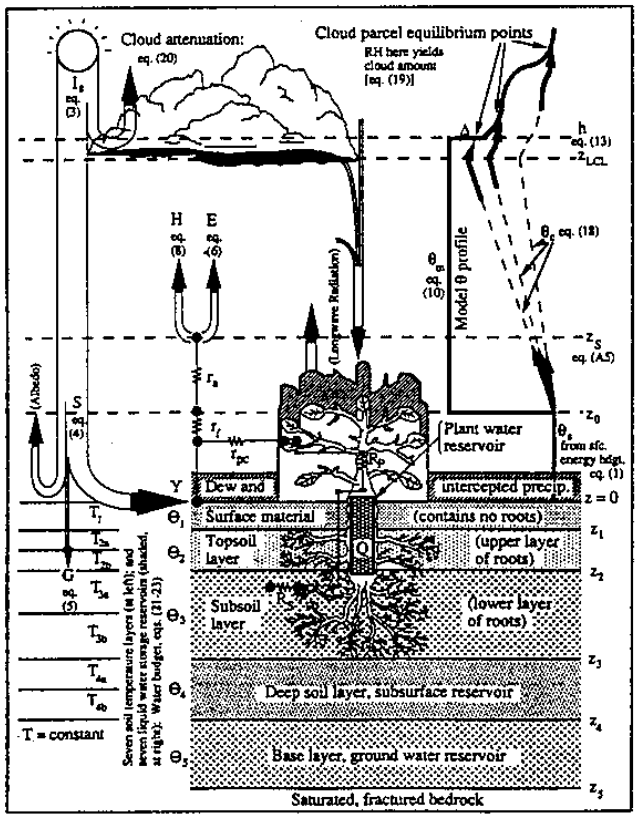

Fig. 2 Schematic representation of the PLACE Model domain. (See text for more details.)

that PLACE is one of the more stable, accurate models among the two dozen available.

The experiments described herein were produced with 500 m horizontal resolution with periodic lateral boundary conditions, and a stretched vertical coordinate. A 5 km absorbing layer was imposed from 15 - 20 km. Each simulation was run for sixteen hours, assuming an east-west orientation for the two-dimensional domain. The total domain size was 512 km in the horizontal and 20 km in the vertical (Table 1). Two-dimensional simulations have been shown to realistically represent the basic structure of developing convective systems (Rotunno *et al* , 1988; Nicholls and Weissbluth, 1988; Nicholls *et al*, 1991; Tao and Simpson, 1993), and heating and drying rates (Tao and Simpson, 1993; Halverson *et al*, 1995).

Table 1 Model input parameters used for numerical simulations.

Condition	Value
Day of the Year	July 1
Latitude for soil day	28
Latitude for Coriolis	0
Initialization time	6 a.m.
Integration time step	5 s
Simulation length	16 h
Height of the atmosphere	20 km
Number of vertical grid elements	50
Vertical grid resolution (stretched)	5-400 m
Lateral boundary conditions	periodic
Horizontal grid resolution (fixed)	500 m

2.2 *Atmospheric Conditions*

Two soundings, one located on the west coast of Florida and the other on the east coast on July 27, 1991, were taken from

the Convection and Precipitation Electrification Experiment (CaPE) over Florida. They were averaged to obtain a mean sounding for an east-west cross section over the peninsula. Although it had only a small initial CAPE of 740 kJ kg^{-1}, the average sounding had a relatively low lifting condensation level pressure (LCL; 1010 mb), level of free convection (LFC; 839 mb), and high equilibrium level (EL; 190 mb). Thus, upon moistening of the planetary boundary layer, the initial sounding (shown in Figs. 3a and 3b) was conducive to the development of deep moist convection. The maximum speed of the east-west horizontal wind was not large. However, there was low level wind shear, with increasing westerly wind in the lower troposphere. The westerly wind then decreased in the middle troposphere, and became increasing easterlies in the upper troposphere.

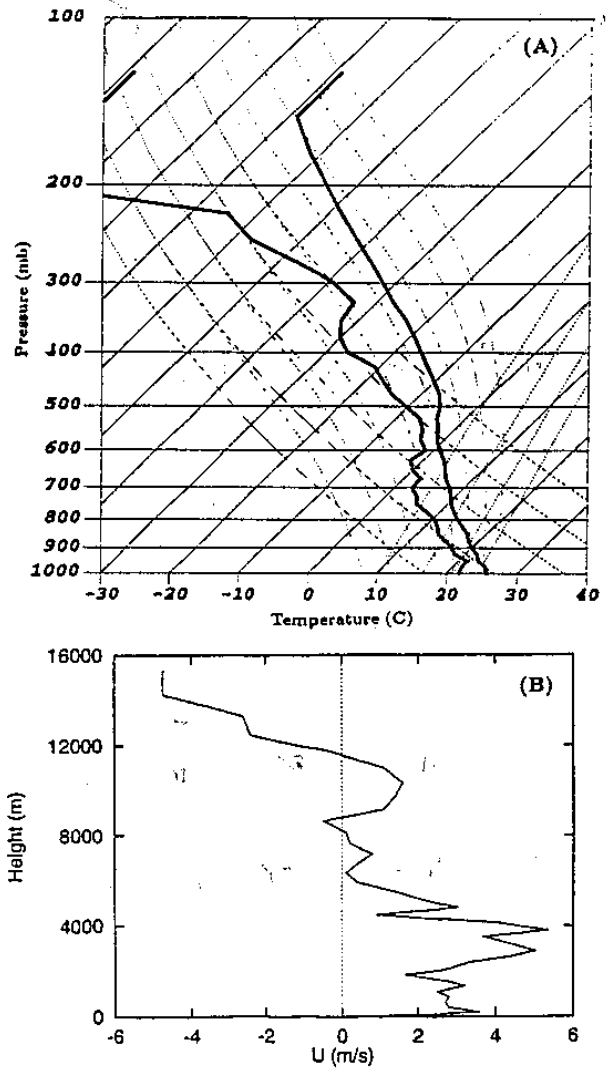

Fig. 3 (a) Atmospheric sounding obtained from the Convective and Precipitation Electrification Experiment (CaPE). (b) Vertical wind profile from the CaPE sounding.

The relatively larger moisture content, high tropopause, and wind profile was indicative of a tropical-like sounding. Because the difference in wind speed between the lower and upper troposphere was about 10 m s^{-1}, there was the potential for the development of stratiform cloud.

2.3 Surface Characteristics

Collins and Avissar (1994) identified the land-surface characteristics as modeled, which have a predominant impact on the turbulent sensible and latent heat fluxes at the ground surface. Based on model simulation results, they found that the most important characteristics were the land surface wetness (the relative availability of soil moisture in the upper soil layer for evaporation), plant stomatal conductance, leaf area index, surface roughness, and albedo. Of these, the stomatal resistance was found to have a predominate role in vegetation during daytime hours and under clear-sky conditions.

The stomatal resistance is a strong function of soil moisture in the root zone. For this reason, the soil moisture of sandy-clay-loam was chosen to *control* the distribution of land surface fluxes from a uniformly distributed homogeneous vegetation consisting of a broad-leaf and coniferous forest (additional soil and vegetation characteristics are described in Table 2). It should be noted, however, that

the modelled soil moisture was interactive with evaporative processes, rainfall, runoff, and drainage during the simulated runs. Thus the stomatal resistance evolved from its initial state, in response to changes in soil moisture, as well as solar flux and atmospheric moisture deficit.

Table 2 Land characteristics used for the numerical simulations.

Land Characteristic	Value
Surface Roughness (m)	1.11
Surface Albedo	0.20
Surface Emissivity	1.00
Soil Texture	sandy-clay-loan
Soil Depth (m)	10
Root Zone Depth (m)	1.6
Porosity ($mm^3\ mm^{-1}$)	0.404
Field Capacity ($mm^3\ mm^{-1}$)	0.298
Wilting Point ($mm^3\ mm^{-1}$)	0.137
Slope of Retention Curve	6.77
Saturated Matric Potential (cm)	-13.49
Saturated Hydraulic Conductivity (cm^{-1})	4.45×10^{-4}
Vegetation	Tall, Broadleaf & Needleleaf Trees
Leaf Area Index	2.46
Minimum Stomatal Resistance (s/m)	1.00
Maximum Stomatal Resistance (s/m)	10.0
Plant Critical Water Potential (m)	-200

2.4 Numerical Simulations

Seven different distributions of soil moisture were specified to create seven domains of alternating dry and wet patches with average length 1 km, 8 km, 16 km, 32 km, 64 km, 128 km, and 256 km, respectively. In the first five of these domains, a random number generator was used to specify the length of individual patches, subject to the constraint that no patches were more than twice the average. It was thought that a random distribution of these patches might produce model fields more realistic than those obtained over uniformly sized patches. In the sixth domain, there were two each of dry and wet patches with length of 128 km. A single dry/wet patch filled the seventh domain, with equal patch length of 256 km. In these last two simulations, the size of the patches were large enough to preclude the need for a random generator. The size of all patches varied in the east-west direction, but were assumed to have infinite length in the north-south direction due to the two-dimensionality of the model domain.

In each of these seven model domains, the mean volumetric soil moisture was 0.22, which was half way between the wilting point and field capacity. Wilting point is the volumetric water content at which plants can no-longer extract water from the soil, while field capacity is the volumetric water content corresponding to a balance that occurs in wet soil between diffusion (up) and gravitational drainage (down). The soil moisture of individual patches (which consisted of grid-elements with similar moisture availability) were chosen to have a soil moisture value of either 0.153 or 0.282. Superimposed on each grid element was a random value of soil wetness.

These seven model domains were run to produce a set of 28 simulations using four different profiles of the background wind. The first profile is that shown in Fig. 3b (hereafter, referred to as BW1), which was obtained as the mean of the two observational soundings. The second wind profile is the same as the initial sounding from the surface up to 3000 m, but above 3000 m the wind was set at 5 $m\ s^{-1}$ from the west

at all model levels (hereafter, BW2). The wind in the third profile was set at 0.5 m s^{-1} from the west at all model levels (hereafter, BW3), while it was set at 5 m s^{-1} from the west in the fourth profile (hereafter, BW4).

3. RESULTS

3.1 Very Large and Very Small Patches

The development of moist convection in Exp. 1 and Exp. 2 was influenced by the different landscapes in each. Contrasted below are the impacts on sensible and latent heat flux, as well as the atmospheric fields within the lower troposphere. The spatial distribution of cloud condensate, the time and spatial distribution of rainfall, and the domain averaged accumulated rainfall are examined in order to document the intensity and spatial distribution of the moist convection.

The initial soil moisture distribution for Exp. 1 is shown in Fig. 4a, for the top soil layer (0.01 m - 0.1 m). The root fraction within this layer was 0.50; thus, the soil moisture in this layer had an important impact on the surface heat fluxes by affecting the energy balance at the leaf surface. There was a 256 km dry patch in the center of the domain in Exp. 1; noting that the lateral boundary conditions were periodic, it was surrounded by a wet patch of the same size. After 9:30 LST, the evaporative demand from the dry soil was larger than the available supply of moisture. Hence, the contiguous dry and moist patches present in Exp. 1 experienced quite different heat fluxes.

The domain of Exp. 2 consisted of a number of very small dry and wet land

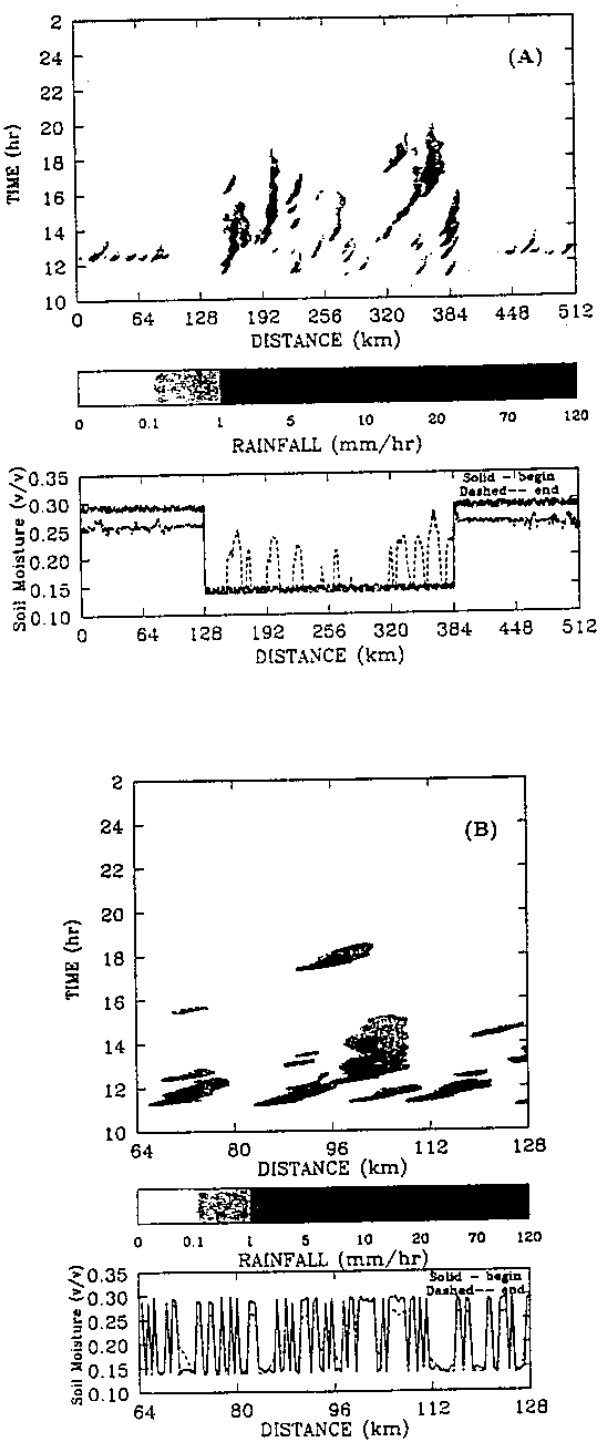

Fig. 4 Spatial distribution of soil moisture (bottom) and time and spatial distribution of rainfall (top) for simulations (**a**) Exp. 1 and (**b**) Exp. 2.

surface patches with an average length of about 1 km (Fig. 4b). In Exp. 2, the dry and wet patches also experienced heat fluxes of different magnitude (Fig. 3 (bottom)). Here, however, the distribution of the fluxes were not contiguous over large horizontal distances.

Because the distribution of heat fluxes in Exp. 1 was different than Exp. 2, the atmospheric fields within the planetary boundary layer (PBL) were also different. In Exp. 1, the PBL above the dry patch was warmer than above the wet patch; thus, the pressure was lower over the dry patch than over the wet patch. For this reason, a mesoscale circulation formed near the edge of the soil moisture discontinuity. A similar mesoscale circulation formed at the downwind (eastern) edge of the dry patch (not shown). The horizontal length-scale of this circulation (and the other) was much larger than its vertical scale, and it was clearly evident in the atmospheric fields. In contrast, horizontal mixing by turbulent-scale processes (both resolved and unresolved) in Exp. 2 precluded the formation of temperature gradients over large horizontal scales. Thus, only Rayleigh-Benard cells were located above the dry land patches in Exp. 2, in response to heating of the surface layer. The horizontal scale of each convective cell was similar to its vertical scale. Note that some of these convective cells were also obtained in Exp. 1.

At 11 LST, a shallow convective cloud (not shown) had formed along the sea-breeze like front in Exp. 1 and the mesoscale circulation had also grown more robust. Model results show that rain cells developed along both sea-breeze fronts. These fronts and their associated moist convection than moved over the dry patch away from the soil moisture discontinuities. The convection along both fronts dissipated before the convergence of these fronts.

At 11 LST, shallow convective clouds had also formed in the domain of Exp. 2 (not shown). Here, however, rain cells were relatively short-lived and were associated with small-scale perturbations in the horizontal wind field. These small-scale perturbations were the surface winds associated with the Rayleigh-Benard cells. It was also interesting to note that the horizontal scale of the rain cells were much larger in Exp. 1 than Exp. 2, owing to formation of rain behind the sea-breeze like fronts in the former.

Figure 5 shows the time and spatial cross-section of CAPE obtained in Exp. 1. Utilizing one-dimensional modeling results, Segal *etal* (1995) and Clark and Arrit (1995) found that the largest potential for deep convection occurs over moist soils (or fully transpiring vegetation). Thus, it was quite interesting that the most intense and long-lived rainfall occurred along the sea-breeze like fronts because the wet patch, not the sea-breeze like fronts, was the location of the largest CAPE. This is because the fronts were the location of continuous forcing, *ie* precipitation was sustained along these fronts by positive temperature and moisture advection.

The Rayleigh-Benard cells over both the dry patch (between the sea-breeze like fronts) and the wet patch were short lived. The rainfall occurred first over the dry patch and then over the wet patch - after Rayleigh-Benard convection occurred over each. In this case, the atmosphere over both patches was susceptible to moist convection; but a trigger was required to initiate the moist convection. There was no discernable difference in the precipitation

over each; probably because the atmosphere was initially quite moist.

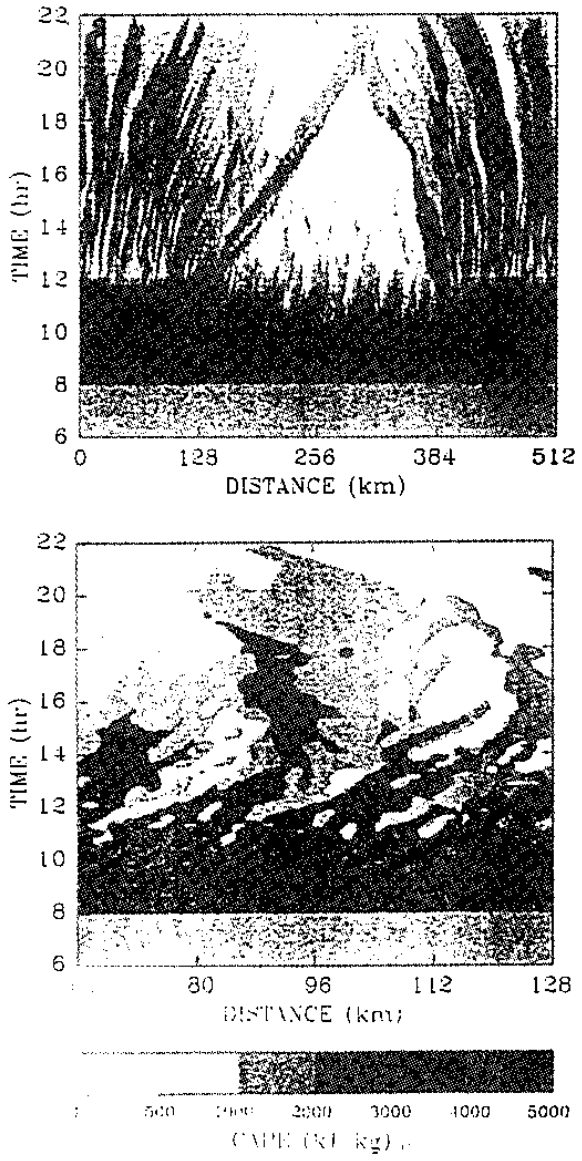

Fig. 5 Spatial and time distribution of Convective Available Potential Energy obtained for Exp. 1 (top) and Exp. 2 (bottom).

In Exp. 2, the association between rainfall and the CAPE was tenuous. The largest CAPE occurred in this simulation over the wet patches. However, the rainfall occurred near the edge of the soil moisture discontinuities (Fig. 4b), in response to the Rayleigh-Benard cells generated by the surface heating over the small dry patches. This further suggests that if the atmosphere is initially quite moist, the development of moist convection requires the triggering by turbulent convection - not further moistening of the planetary boundary layer. Conversely, if the atmosphere is relatively dry, moist convection might occur first over the wet ground, and then, perhaps, later over the dry ground - even though turbulence is more intense over the latter.

The rainfall obtained in Exp. 1 and Exp. 2 were like *footprints* on the land surface, which can have an important impact on soil moisture distribution by the end of the numerical simulation. For example, rainfall on the dry patch in Exp. 1 led to a significant change in the soil moisture distribution of the dry patch. In some grid-elements, the soil moisture became similar to that of the wet patch. Thus, new soil moisture discontinuities, and hence new patch sizes, were created by the rainfall footprints.

The soil moisture distribution at the end of Exp. 2 is shown in Fig. 4b, for a subsection of the domain. It is seen that rainfall occurred along the edge of the wet patches, and that the length-scale of some of the wet patches have grown to resemble the length-scale of the rainfall footprints.

Note, however, that the size of the new patches after one simulation day were much different in Exp. 1 than in Exp. 2. Moreover, the time-scale of the moist convection in both simulations was much less than the time-scale required for the soil moisture distribution to fully reflect the horizontal scale of rainfall footprints. That is, for some type of equilibrium to be reached between

rainfall and soil moisture distribution. For this reason, multiday simulations were produced to examine the time dependence of landscape patches. The results from these simulations are discussed in a future paper (Lynn *et al*, 1996a).

3.2 Impact of Background Wind

The profiles of mean, background wind in Exp. 1 and Exps. 3-5 were affected by the surface layer momentum flux and vertical transports. For this reason, it was useful to examine the profiles of wind for each, just prior to the formation of moist convection (at 11 LST), to look for any significant changes in each of them. Figure 11 shows that the momentum flux acted to reduce the low level westerly wind in each, such that the wind varied nearly linearly and increasing within the PBL. Otherwise, there was relatively little change in these profiles, and they were quite different from each other.

An analysis of model results indicated that the intensity, horizontal scale, duration, and propagation speed of the rain cells were very sensitive to the profile of background wind. For example, an eastward moving and long-lived line of rain cells was obtained in Exp. 3 (BW2). In contrast, only relatively weak, discrete rain cells with small horizontal scale and small propogation speed were obtained in Exp. 4 (BW3). In Exp. 5 (BW4), there was also a line of moist convection that propagated across the domain.

The initial development of moist convection in Exp. 4 was quite weak. This was because the eastward propogation of the sea-breeze like front in a light background wind was quite slow, resulting in reduced lifting along this front. Hence, it took until about 1300 LST before a more intense convective cell fo formed. Here, as in Exp. 3, the developing cloud aloft remained coupled to the convective cloud below, and there was relatively little inflow into this cloud aloft. Thus, strong middle and upper level convection did not take place, and the frontal zone was not strengthened by the development of a cold pool. Moreover, the propogation speed of the sea-breeze like front was faster than the speed of the convective cells. Thus, the frontal forcing moved far downwind of the upwind convective cells and they soon dissipated.

Finally, the development of rain cells in Exp. 4 and Exp. 5 were more intense on the western edge of the dry patch than the eastern edge. This is in contrast to Exp. 1, in which the development of rainfall was relatively symmetric about the dry patch. In each experiment, rain cells developed on the eastern side of the dry patch along the westward propagating front. However, in Exp. 4 and Exp. 5 these rain cells were advected by the mean westerly wind away from the westward propagating sea-breeze like front. Thus, the forcing by the westward moving fronts in Exp. 4 and Exp. 5 was relatively divorced from the developing convective cells on the eastern side of the patch. This precluded significant intensification of these rain cells.

3.3 Impact of Stability

Exp. 6 was produced with the soil moisture distribution and profiles of temperature and moisture obtained at the end of Exp. 1 (after running this experiment until 6 LST on day 2). The new temperature profile was quite stable (a result of the previous day's convection), although more moist than the previous day. Because this profile was quite stable the CAPE was relatively small, even though the profile was more moist. Only weak, relatively shallow moist convection developed in this

experiment and the accumulated rainfall was only 0.45 mm, which was much less than in Exp. 1. This was despite the additional surface forcing provided by additional patches, with approximately an average size of 32~km, that were located within the original dry patch.

This simulation represents, in a sense, an extreme case because the initial profiles were quite changed from their values on day 1. If advection and gravity waves were allowed (by the boundary conditions) to exchange energy out of the domain, then the results might have been quite different. For example, an additional simulation (Exp. 7), which reflected only changes in the soil moisture distribution, resulted in a total accumulation of rainfall equal to 2.27 mm (compared with 2.77 mm for Exp. 1).

Acknowledgement

The first Author is supported by the NASA Headquarters physical climate program, the NASA TRMM, and the interdisciplinary program of EOS. The second author was supported by a National Aeronautics and Space Administration fellowship provided through the Universities Space Research Association (NAS532484). We thank Dr. Joanne Simpson, Dr. Franco Einaudi and Dr. Robert Adler for their support. We wish to thank Dr. Max Suarez, Dr. Peter Wetzel and Dr. Yansen Wang for valuable advice, and Aaron Boone for helping to implement the PLACE model in GCE model.